R-Type Ca^{2+} Channels Are Coupled to the Rapid Component of Secretion in Mouse Adrenal Slice Chromaffin Cells

Almudena Albillos,[1,2] Erwin Neher,[1] and Tobias Moser[1,3]

[1]*Department of Membrane Biophysics, Max-Planck Institute for Biophysical Chemistry, 37077 Goettingen, Germany,* [2]*Instituto de Farmacología Teófilo Hernando, Departamento de Farmacología y Terapeútica, Facultad de Medicina, Universidad Autónoma de Madrid, 28029 Madrid, Spain, and* [3]*Department of Otolaryngology, Goettingen University Medical School, 37073 Goettingen, Germany*

Patch-clamp measurements of Ca^{2+} currents and membrane capacitance were performed on slices of mouse adrenal glands, using the perforated-patch configuration of the patch-clamp technique. These recording conditions are much closer to the *in vivo* situation than those used so far in most electrophysiological studies in adrenal chromaffin cells (isolated cells maintained in culture and whole-cell configuration). We observed profound discrepancies in the quantities of Ca^{2+} channel subtypes (P-, Q-, N-, and L-type Ca^{2+} channels) described for isolated mouse chromaffin cells maintained in culture. Differences with respect to previous studies may be attributable not only to culture conditions, but also to the patch-clamp configuration used. Our experiments revealed the presence of a Ca^{2+} channel subtype never before described in chromaffin cells, a toxin and dihydropyridine-resistant Ca^{2+} channel with fast inactivation kinetics, similar to the R-type Ca^{2+} channel described in neurons. This channel contributes 22% to the total Ca^{2+} current and controls 55% of the rapid secretory response evoked by short depolarizing pulses. Our results indicate that R-type Ca^{2+} channels are in close proximity with the exocytotic machinery to rapidly regulate the secretory process.

Key words: calcium channels; exocytosis; membrane capacitance measurements; adrenal slice; chromaffin cell; calcium-secretion coupling

During the last two decades, great efforts have been made to characterize the variety of voltage-dependent Ca^{2+} channels in excitable cells, using molecular, biophysical, and pharmacological approaches. The availability of toxins to dissect different components of Ca^{2+} currents has helped in the characterization of different types of Ca^{2+} channels, but it has also created some uncertainties. Pharmacologically, neuronal high voltage-activated Ca^{2+} channels have been classified as dihydropyridine (DHP)-sensitive (L-type channels), ω-conotoxin GVIA-sensitive (N-type channels), and ω-agatoxin IVA-sensitive (P channels with $K_d < 10$ nM, and Q channels with $K_d > 10$ nM) (Mintz et al., 1992b; Sather et al., 1993; Randall and Tsien, 1995). A current resistant to DHP, ω-conotoxin MVIIC, and ω-agatoxin IVA has been named R-type (Zhang et al., 1993; Randall et al., 1995; Tottene et al., 1996; Magnelli et al., 1998).

Adrenal medullary chromaffin cells of various mammalian species have been shown to express Ca^{2+} channels of the L-subtype (Hoshi and Smith, 1987; Bossu et al., 1991a,b; Albillos et al., 1994), N- subtype (Hans et al., 1990; Bossu et al., 1991a,b; Artalejo et al., 1992; Albillos et al., 1994), P-subtype (Gandía et al., 1993; Albillos et al., 1993; Artalejo et al., 1994), and Q-subtype (López et al., 1994; Albillos et al., 1996). These previous studies on Ca^{2+} channel currents have been performed in the whole-cell configuration of the patch-clamp technique on primary cultures of chromaffin cells, mostly using Ba^{2+} as a charge carrier. However, these cells may suffer drastic changes in their functional properties after several days in culture. In fact, chromaffin cells of acutely prepared mouse adrenal slices exhibit a prominent fast secretory component that is hardly detected in primary cell cultures (Moser and Neher, 1997). It is, therefore, plausible that chromaffin cells in acutely prepared slices might express Ca^{2+} channel subtypes different from those described up to now for isolated cells maintained in culture. Here, we have pharmacologically separated the various subcomponents of the whole-cell Ca^{2+} current (I_{Ca}) present in chromaffin cells of mouse adrenal slices. To achieve conditions as close as possible to the physiological ones, we have used the physiological Ca^{2+} concentration and the perforated-patch configuration, which preserves the cytosolic cellular composition. We have found in this preparation, although in different proportions, all Ca^{2+} channel subtypes that had been previously described for mouse adrenal chromaffin cells in culture (Hernández-Guijo et al., 1998). Most importantly, we report for the first time an R-type Ca^{2+} channel current that contributes substantially to the rapid secretory response in mouse adrenal slices, measured with capacitance techniques.

MATERIALS AND METHODS

Adrenal slice preparation and solutions. Mouse adrenal slices were prepared as previously described (Moser and Neher, 1997). Slices were kept at 37°C in a holding chamber containing solution 1 bubbled with 95% O_2 and 5% CO_2.

Two bicarbonate-buffered saline (BBS) solutions with different concentrations of $CaCl_2$ were used. The standard BBS solution or solution 1 contained (in mM): 2 $CaCl_2$, 125 NaCl, 26 $NaHCO_3$, 2.5 KCl, 1.25 NaH_2PO_4, 1 $MgCl_2$, and 10 glucose. Solution 2, which was used for slice preparation, was identical to solution 1, except that it contained 0.1 mM $CaCl_2$ and 3 mM $MgCl_2$.

For electrophysiological recordings, solution 1 containing 0.2 mM D-tubocurarine and 5 μM TTX (or 10 μM, unless otherwise stated) was perfused extracellularly at a rate of 1–2 ml/min. In some experiments, $CaCl_2$ was omitted, and 2 mM EGTA was present. All BBS solutions were adjusted to pH 7.4 by bubbling with 95% O_2 and 5% CO_2.

The pipette solution contained (in mM): 145 Cs-Glutamate, 8 NaCl, 1 $MgCl_2$, 10 HEPES, and 0.5 mg/ml amphotericin B. The pH of the perforated-patch solution was adjusted to 7.2 with CsOH. All chemicals were obtained from Sigma (St. Louis, MO) with the exceptions of CsOH (Aldrich, Milwaukee, WI) and amphotericin B (Calbiochem-Novabiochem, La Jolla, CA). An amphotericin B stock solution was prepared every day at a concentration of 50 mg/ml in DMSO and kept protected from light. The final concentration of amphotericin B was prepared by ultrasonicating in the darkness 10 μl of stock amphotericin B and 1 ml of CsGlutamate internal solution. Pipettes were tip-dipped in amphotericin-free solution for several seconds and back-filled with freshly mixed amphotericin intracellular solution.

Received June 9, 2000; revised Sept. 5, 2000; accepted Sept. 6, 2000.

This work was supported by grants from the Deutsche Forschungsgemeinschaft (SFB 523/B4) to E.N. and T.M.. We thank Dr. Corey Smith for his help on writing the macros to analyze data, Dr. Antonio G. García for his encouragement and critical feedback along this study, and Drs. Jose María Trifaró, Emilio Carbone, and Robert Burgoyne for critical reading of this manuscript.

Correspondence should be addressed to Dr. Almudena Albillos, Instituto de Farmacología Teófilo Hernando, Departamento de Farmacología y Terapeútica, Facultad de Medicina, Universidad Autónoma de Madrid, c/Arzobispo Morcillo 4, 28029 Madrid, Spain. E-mail: almudena.albillos@uam.es.

 0270-6474/00/208323-08$15.00/0

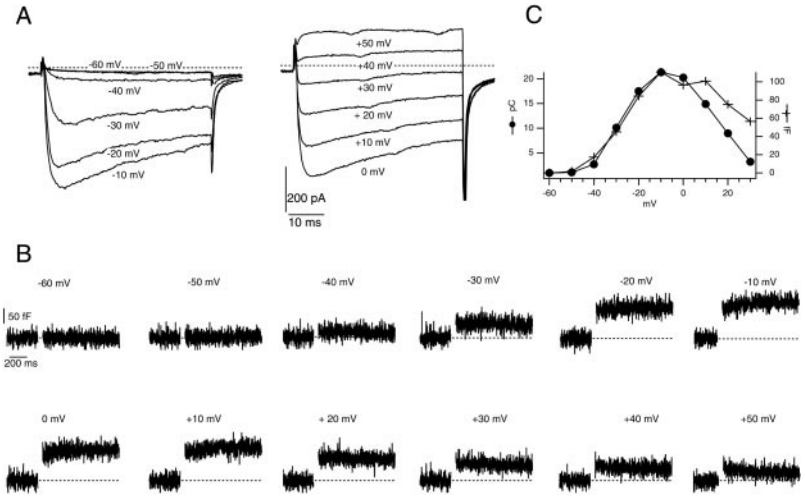

Figure 1. Voltage dependence of Ca^{2+} currents and secretion in mouse adrenal slice chromaffin cells. Ca^{2+} currents and capacitance changes were recorded in the presence of 5 μM TTX and 2 mM Ca^{2+} at different voltages. *A,* Ca^{2+} currents ($V_h = -70$ mV), evoked by depolarizing test potentials, as indicated. *B,* Corresponding C_m traces. *C,* Plot of ΔC_m (*ordinate, right*) and Q_{Ca} (*ordinate, left*) versus the potential. ΔC_m reached peak values at the same voltage as Q_{Ca}, and both declined above that potential.

Isolation and culture of mouse chromaffin cells and solutions. Mouse chromaffin cells were isolated according to the method used by Hernández-Guijo et al. (1998). Cells were used after 1 or 2 d in culture.

The BBS-based recording solution consisted of solution 1 containing 0.2 mM D-tubocurarine and 5 μM TTX. The HEPES-based recording solution had the following composition (in mM): 2 $CaCl_2$, 145 NaCl, 5.5 KCl, 1 $MgCl_2$, 10 HEPES, and 10 glucose.

The pipette solution in the perforated-patch configuration was the same as the one used in adrenal slice cells. In the whole-cell configuration, it contained (in mM): 100 CsCl, 10 NaCl, 20 TEACl, 14 EGTA, 20 HEPES, 5 MgATP, 0.3 and Na_2GTP.

Electrophysiological measurements in chromaffin cells in situ. Slices were fixed in the recording chamber by means of a grid of nylon threads. After the chamber containing the slices was mounted onto the stage of an upright microscope (Axioscope; Zeiss), the chamber was perfused with bubbled BBS (solution 1). The perfusion system for application of drugs consisted of a multibarrelled glass pipette positioned close to the cell under study. Five stainless steel needles inside the pipette allowed the local perfusion of solutions, and these were fed by means of Teflon syringes and tubes, each of them used only for a particular drug to avoid any contamination of solutions (Carbone and Lux, 1987). Before establishing a gigaseal, loose material from the cell surface was removed with a cleaning pipette.

Elecrophysiological measurements were performed using an EPC-9 amplifier and PULSE software running on an Apple Macintosh. Pipettes of 1–3 MΩ resistance were pulled from borosilicate glass capillary tubes, partially coated with a silicone compound (G. E. Silicones, Bergen Op Zoom, The Netherlands), and fire-polished. After seal formation and perforation, access resistance ranged from 8 to 20 MΩ. Cell membrane capacitance (C_m) changes were estimated by the Lindau-Neher technique (for review, see Gillis, 1995) implemented as "Sine + DC" feature of the "Pulse" lock-in software. A 1 kHz, 70 mV peak-to-peak amplitude sine wave was applied to a holding potential of −70 mV. Capacitance increments caused by depolarizations were determined from the high time resolution "Pulse" data, as the difference between average cell capacitance measured in a 300 msec window, before and after the depolarization. The data during the first 100 msec after the depolarization were neglected to avoid the influence of nonsecretory capacitance changes (Horrigan and Bookman, 1994). Between stimulations, capacitance data were recorded at low time resolution using the X-chart plug-in module of the Pulse software. The X-chart module sampled all experimental parameters at 9 Hz.

Step depolarizing pulses from a holding potential of −70 mV were used to evoke Ca^{2+} currents. After the depolarizing pulse, the potential returned to −50 mV for 15 msec to better analyze the deactivation phase of the current. Currents were filtered at 2 kHz and sampled at 12 kHz. First, a ramp protocol was applied to determine the peak Ca^{2+} current potential, which ranged from −10 to +10 mV. Only cells with resting currents <20 pA were analyzed. No leakage correction was performed. No liquid junction potential correction was used, because of uncertainties about its merits when the perforated-patch configuration is used. K^+ currents were blocked by intracellular Cs^+ and extracellular D-tubocurarine (Park, 1994). Tetrodotoxin was used to block Na^+ channels. The transient nonsecretory capacitance change (ΔC_t) observed after depolarization of rat chromaffin cells (Horrigan and Bookman, 1994) was measured during perfusion with solution 1 containing no Ca^{2+} and 2 mM EGTA. This transient was found to be absent ($n = 6$) or to exhibit a τ of 10 msec in one cell and 188 msec in a different cell. The analysis of the data were conducted on a Macintosh computer using IgorPro (Wavemetrics, Lake Oswego, OR). Unless otherwise stated, data are given as means ± SE.

Electrophysiological measurements in isolated cultured chromaffin cells. Ca^{2+} currents were recorded with borosilicate glass electrodes of 2–4 MΩ resistance, mounted on the headstage of a Dagan PC-ONE patch-clamp amplifier. Step depolarizing pulses to 0 mV from a holding potential (V_h) of −70 mV were applied for 50 msec to evoke Ca^{2+} currents. Currents were filtered at 3 kHz and sampled at 12.5 kHz. Only cells with resting currents of <5 pA were used. No leakage correction was performed. An Instrutech ITC-16 controlled by a Macintosh Power PC 8200/120 running Igor (Wavemetrics), and the Pulse Control XOPs (J. Herrington and R. J. Bookman, University of Miami, Miami, FL) were used as acquisition system. The analysis of the data were conducted on a Macintosh computer using IgorPro (Wavemetrics). Unless otherwise stated, data are given as means ± SE.

RESULTS

Voltage dependence of I_{Ca} and secretion in chromaffin cells of mouse adrenal slices

The voltage dependence of Ca^{2+} currents and secretion was first characterized. Figure 1*A* shows original traces of I_{Ca} recorded in the presence of TTX at potentials increasing from −60 to +50 mV. The Ca^{2+} current started to activate at approximately −40 mV, peaked at −10 mV, and reversed at 30 mV. Note some notch-like currents on top of the Ca^{2+} currents. These are attributable to action potentials of neighboring cells coupled with low conductance to the patch-clamped cell (Moser, 1998). The corresponding C_m traces for the individual depolarizations are shown in Figure 1*B*. The blank spaces in the C_m records correspond to the 50 msec depolarizing pulses, during which C_m could not be measured because of nonlinear conductance changes. Increments in capacitance became visible at −40 mV, increased with rising voltages up to −10 mV, and finally decreased beyond this potential. *I–V* curves for the time integral of I_{Ca} (Q_{Ca}), and for the ΔC_m, thus, showed a similar bell-shaped voltage dependence up to 30 mV (Fig. 1*C*). The presence of T-type Ca^{2+} channels was explored by holding the potential at −100 mV and applying either a ramp protocol from −100 to 60 mV or a single pulse to −50 mV. Under these conditions, no indication of the presence of this type of Ca^{2+} channel was found in 15 cells tested (data not shown).

P and "Q-like" Ca^{2+} channels in chromaffin cells of mouse adrenal slices

The presence of P- and Q-type Ca^{2+} channels was determined by local perfusion with ω-agatoxin IVA (ω-Aga-IVA). This toxin blocks P-type channels with an IC_{50} of 2 nM (Mintz et al., 1992b; Randall and Tsien, 1995) and Q-type channels with an IC_{50} of 90–200 nM (Sather et al., 1993; Randall and Tsien, 1995). To test the effects of the toxin on I_{Ca}, we measured the current in response to depolarizing pulses of 50 msec duration. Pulses were applied to the peak current potential. Typical experiments are presented in Figure 2. Figure 2*A* displays the effects of the toxin on the current amplitude measured at the end of the depolarizing pulse (I_{final}). In the presence of low concentrations of the toxin (20 nM), I_{final} was blocked by 34%, from 505 to 331 pA. Subsequent perfusion with 2 μM toxin, to assay for the presence of Q-type channels, caused an additional blockade of 28%. In nine cells tested, P-type Ca^{2+}

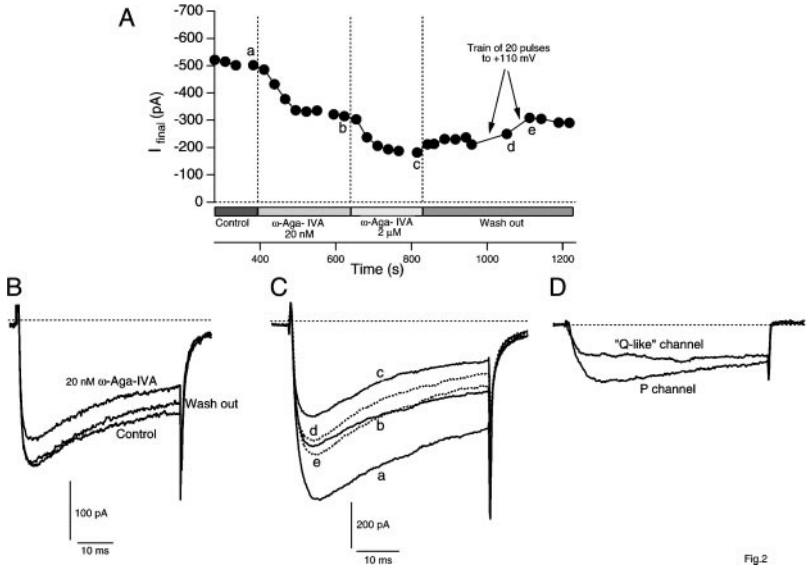

Fig.2

Figure 2. P- and "Q-like"-type channels are present in mouse chromaffin cells of adrenal slices. *A,* Time course of Ca^{2+} currents measured at the end of 50 msec depolarizing pulses applied every 30 sec to 0 mV from a holding potential of −70 mV. The selective blockade of P-type channels was achieved by perfusion with 20 nM ω-Aga-IVA. Q-type channels were subsequently blocked by perfusion with 2 μM ω-Aga-IVA. After wash out, the recovery was hastened by application of two trains of 20 pulses to +110 mV. Blank spaces in the record were caused by ramp voltage protocols applied at those points. *B,* Reversibility of P-type channel blockade in a different chromaffin cell. After a steady-state was reached in control conditions (*Control* trace), 20 nM ω-Aga-IVA was perfused (ω-Aga-IVA trace), and the subsequent wash out led to an almost complete recovery of the Ca^{2+} current from the blockade (*Wash out* trace). *C, D,* Kinetics of inactivation of ω-Aga-IVA-sensitive Ca^{2+} channels. Traces *a* (control), *b* (in the presence of 20 nM ω-Aga-IVA), *c* (in the presence of 2 μM ω-Aga-IVA), *d* (after wash out), and *e* (wash out after two trains of 20 pulses to +110 mV) from the cell of *A*, are plotted in *C*. The P channel was obtained as the difference between the control trace and the 20 nM ω-Aga-IVA trace (*a, b*). The "Q-like" channel was obtained as the difference between *b* and *c* traces. The P channel exhibited a slow inactivation, whereas the "Q-like" channel did not inactivate at all.

channels accounted for 22.4 ± 4% of the total current. Q-type Ca^{2+} channels represented a similar amount, 22.6 ± 7% ($n = 6$ cells). The contributions were estimated as the difference between the blockade of I_{final} by high and low concentrations of the toxin.

The blockade of P-type Ca^{2+} channels by 20 nM ω-Aga-IVA was partially reversible ($n = 4$ cells), as shown in a different cell in Figure 2*B*. The partial recovery from the 2 μM ω-Aga-IVA-induced inhibition was probably attributable to the reversibility of the blockade of P-type channels. The recovery from the 2 μM ω-Aga-IVA-induced blockade was hastened by strong depolarizing pulses, as shown for the ω-Aga-IVA-induced blockade in cerebellar Purkinje cells (Mintz et al., 1992a), in cerebellar granule cells (Randall and Tsien, 1995), and in currents supported by α_{1A} subunits expressed in *Xenopus* oocytes, which resemble Q-type currents in cerebellar granule neurons (Sather et al., 1993).

Figure 2*C* shows original traces of control Ca^{2+} current (*trace a*), after application of 20 nM (*trace b*) and 2 μM ω-Aga-IVA (*trace c*), as well as wash out before (*trace d*) and after (*trace e*) two trains of depolarizing pulses. The current mediated by P channels (calculated as the difference between *traces a* and *b*) either did not inactivate or exhibited only slight inactivation ($n = 6$ cells), similar to what was found in neurons (Usowicz et al., 1992; Randall and Tsien, 1995). The Q-type Ca^{2+} current (difference between *traces b* and *c* in Fig. 2*D*) did not inactivate at all ($n = 6$ cells). However, α_{1A} channels expressed in *Xenopus* oocytes were prominently inactivating (Sather et al., 1993), as well as Q-type Ca^{2+} channels in neuronal cells (Randall and Tsien, 1995). Nevertheless, on the basis of their pharmacology, we consider these channels as "Q-like"-type Ca^{2+} channels.

N- and L-type Ca^{2+} channels in chromaffin cells of mouse adrenal slices

Following the same protocol as in Figure 2, 1 μM ω-conotoxin GVIA (ω-CTx-GVIA) was used to block N-type Ca^{2+} channels. The temporal course of the inhibition of this channel is shown in Figure 3*A*. The initial current in this cell was 320 pA and decreased by 49% after application of the toxin. Forty percent of the blockade was reversible, in contrast to the blockade of the N-type Ca^{2+} channel in neurons that is considered to be irreversible. Perfusion with a Ca^{2+}-free solution containing 2 mM EGTA diminished the current to 10 pA, which was reversible after wash out. Original traces of control (*trace a*), after ω-CTx-GVIA application (*trace b*), and wash out (*trace c*) are shown in Figure 3*B*. In 12 cells tested, the toxin decreased Ca^{2+} current by 35 ± 5%, with 47 ± 9% of that blockade being reversible ($n = 5$ cells).

The dihydropyridine nifedipine (Nife) at 3 μM, a selective L channel blocker, inhibited 27 ± 4% of the current elicited by 50 msec depolarizing pulses ($n = 13$ cells). This blockade was totally reversible, as shown in Figure 3*C*. Original Ca^{2+} current traces before (*trace a*), in the presence of (*trace b*), and after dihydropyridine application (*trace c*) are shown in Figure 3*D*. In this cell, the blockade by Nife corresponded to 20.4% of the total I_{Ca}.

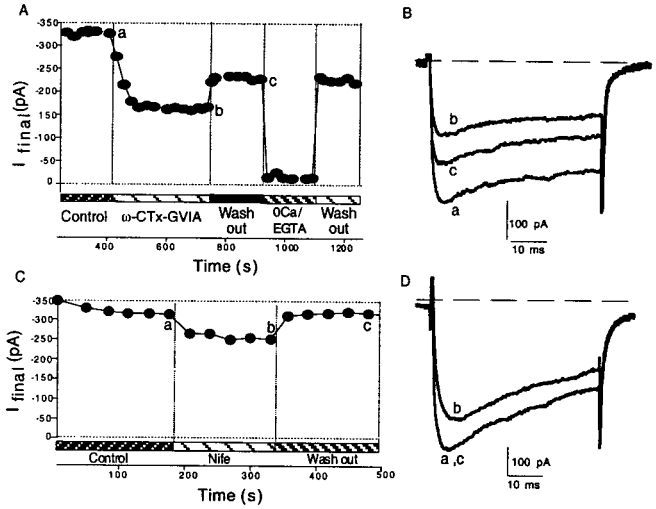

Figure 3. N- and L-type Ca^{2+} channels are present in mouse chromaffin cells in adrenal slices. *A,* Time course of inhibition and recovery of Ca^{2+} currents during application of 1 μM ω-CTx-GVIA to a voltage-clamped mouse chromaffin cell. Perfusion with control solution but in the absence of Ca^{2+} (0 mM Ca^{2+}-2 mM EGTA) led to a rapid abolition of Ca^{2+} currents. Blank spaces in the record were caused by ramp voltage protocols applied at those points. *B,* Original traces before (*trace a*), in the presence of ω-CTx-GVIA (*trace b*), and after wash out (*trace c*), from the same cell as *A*. Note the partial recovery of the ω-CTx-GVIA blockade. *C,* Time course of inhibition and recovery of Ca^{2+} currents during application of 3 μM Nife. *D,* Original traces before (*trace a*), at the end of Nife application (*trace b*), and after wash out (*trace c*), from the same cell as *C*.

The resistant Ca^{2+} channel and its role in secretion in chromaffin cells of mouse adrenal slices

Two different protocols were used to investigate the presence of a channel resistant to blockade by known Ca^{2+} antagonists. The first protocol was applied to four cells and consisted of the sequential addition of toxins (Fig. 4*A*). After the control current reached a steady-state (Fig. 4*A, control trace*), the preparation was perfused with the following drugs, adding each drug cumulatively, to prevent wash out of any Ca^{2+} channel blocker: 20 nM ω-Aga-IVA to block

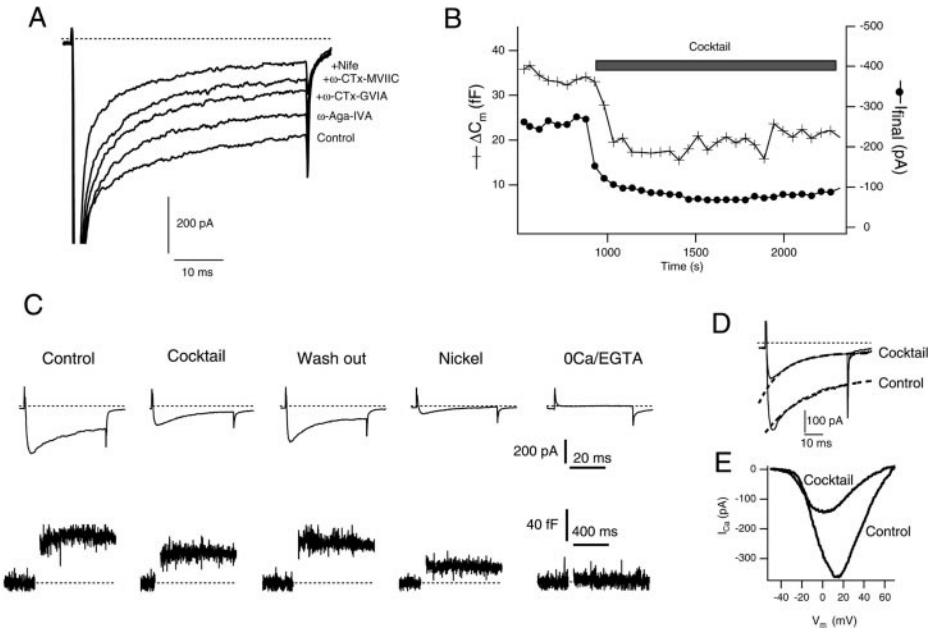

Figure 4. A Ca^{2+} channel current resistant to blockade mediates rapid secretory responses. In *A*, Ca^{2+} channel blockers (20 nM ω-Aga-IVA, 1 μM ω-CTx-GVIA, 3 μM ω-CTx-MVIIC, and 3 μM Nife) were added sequentially, as indicated to the *right* of each trace. No TTX was used in this experiment. Each compound was locally perfused onto the patched cell for ~10 min. In *B*, blockers were added in a different cell simultaneously, as indicated by the *top horizontal bar* (cocktail: 2 μM ω-Aga-IVA, 1 μM ω-CTx-GVIA, 3 μM ω-CTx-MVIIC, and 3 μM Nife). The temporal course of blockade of Ca^{2+} currents (I_{final}) and secretion (ΔC_m) by the cocktail of blockers is shown in this panel. Pulses were applied every minute. *C,* Original recordings of both ΔC_m, and the corresponding I_{final} are shown for the sequential application of control solution, cocktail of blockers, wash out of the cocktail, 5 mM $NiCl_2$, and Ca^{2+}-free–2 mM EGTA in a different cell. *D,* The residual Ca^{2+} current exhibited rapid inactivation kinetics. The inactivation phases of control current and the current elicited after addition of the cocktail of blockers were well fitted with a single exponential function with τ_I = 24 and 14 msec, respectively. *E,* Voltage ramps from −120 to +60 mV were applied after currents had reached a steady-state with control and cocktail solutions. The ramp duration was 50 msec. They were corrected for leakage currents by subtracting the ramp in the presence of 200 μM $CdCl_2$. The concentration of TTX in the experiments of *B–E* was 10 μM to ensure the blockade of Na^+ channels.

P-type Ca^{2+} channels; 7 min later, 1 μM ω-CTx-GVIA was added to block N-type Ca^{2+} channels (perfusion time of ω-Aga-IVA plus ω-CTx-GVIA, 10 min); then, 3 μM ω-conotoxin MVIIC (ω-CTx-MVIIC) was included to target Q-type Ca^{2+} channels and to assure the complete blockade of N- and P-type Ca^{2+} channels, because ω-CTx-MVIIC blocks N- (Swartz et al., 1993; Grantham et al., 1994), P- (Hillyard et al., 1992), and Q-type Ca^{2+} channels (Sather et al., 1993; Randall et al., 1995); finally, after 8 min perfusion with ω-Aga-IVA plus ω-CTx-GVIA plus ω-CTx-MVIIC, 3 μM Nife was added to block L-type Ca^{2+} channels (perfusion time of ω-Aga-IVA plus ω-CTx-GVIA plus ω-CTx-MVIIC plus Nife, 10 min). In the cell shown in Figure 4*A*, P-, N-, Q-, and L- type channels accounted for 28, 19.6, 11, and 18.5% of the total current, respectively. However, in spite of the long time of local perfusion with the different blockers, 23% of I_{final} was still present. This value was 28, 16, and 19% in three other cells to which the same protocol was applied. It should be noted that I_{Ca} was stable for long periods of time because of the use of the perforated-patch configuration.

The second protocol consisted of the perfusion of the whole cocktail of toxins at the same time (n = 7 cells) (Fig. 4*B–E*). Although high concentrations of ω-CTX-GVIA (1 μM), ω-CTX-MVIIC (3 μM), and Nife (3 μM) should be sufficient to block N-, P/Q-, and L-type Ca^{2+} channels, we performed these experiments in the additional presence of 2 μM ω-Aga-IVA to assure a complete blockade of P- and Q-type channels. Depolarizing pulses of 50 msec duration to the peak Ca^{2+} current potential were applied every 30 sec or 1 min to measure simultaneously Ca^{2+} currents and secretion. Under control conditions, depolarizing pulses of 50 msec duration evoked a secretory response of 63.4 ± 9 fF (n = 20 cells). Typical time courses of ΔC_m and I_{final} are shown in Figure 4*B*. The cocktail of toxins blocked maximally Ca^{2+} currents and secretion after 7 min of fast perfusion. In this cell, the resistant Ca^{2+} current corresponded to 24% of the total current, when it was measured at the end of the pulse (I_{final}). The remaining secretory response was 67% of the initial secretion. Figure 4*C* shows details of Ca^{2+} currents and cell membrane capacitance in a different cell where 5 mM $NiCl_2$ and a Ca^{2+}-free solution were applied after wash out of the cocktail. The resistant current in this case amounted to 41% (I_{peak}), and 26% (I_{final}) of the total current. The blockade was partially reversible after washing out the cocktail. A parallel depression of secretion of 35% was observed during the perfusion with the cocktail, and ~50% of this inhibition recovered during the wash out period. Therefore, 65% of the total secretion is related to the resistant component of the current, which contributed only 26% to the whole Ca^{2+} current. On average, the resistant current after the blockade by the cocktail was 34 ± 2.5% (n = 6 cells) and 22 ± 2.6% (n = 11 cells), when measured at the peak and at the end of the depolarizing pulse, respectively. The remaining secretion was 54 ± 9% (n = 6 cells).

After washing out the cocktail, application of 5 mM $NiCl_2$ decreased Ca^{2+} currents by a further 18% and also reduced secretion by an additional 30%. Finally, application of a Ca^{2+}-free solution diminished Ca^{2+} currents to 4 pA and abolished secretion completely. In none of the eight cells tested was secretion observed under this experimental condition. The small remaining inward current was most likely caused by Na^+ ions flowing through Ca^{2+} channels. Currents and secretion recovered after addition of extracellular Ca^{2+}.

The resistant current present in chromaffin cells *in situ* exhibited the rapid inactivation kinetics described for this Ca^{2+} current in neurons (Zhang et al., 1993). Figure 4*D* shows the fits to the inactivating phases of control and resistant currents of the same cell as described above, which exhibited τ_i values of 24 and 14 msec, respectively. In 20 cells, Ca^{2+} currents in control conditions inactivated with a τ of 28.2 ± 2.5 msec, whereas the resistant current exhibited a τ_i of 19.5 ± 2.5 msec (n = 8).

A ramp protocol was applied before and after addition of the cocktail, to investigate the voltage dependence of the blockade (Fig. 4*E*). The peak current potential, which under control conditions was at +14 mV, was shifted to 0 mV in the presence of the mixture of L-, N- and P/Q-blockers. The resistant current was activated at approximately −40 mV. The blockade by the cocktail was voltage-dependent, showing a marked depression above −10 mV with respect to more negative voltages: 19, 57, and 76% blockade at −30, −10, and +10 mV, respectively. In 10 cells tested, this blockade corresponded to 32.4 ± 11%, 64.5 ± 4%, and 79 ± 1%, respectively.

Comparison of the relative contribution of each Ca^{2+} channel subtype to the whole-cell Ca^{2+} current recorded in isolated cells versus adrenal slice cells

Figure 5*A* compares the relative contribution to the total current by each type of Ca^{2+} channel found in this study, where 2 mM Ca^{2+}

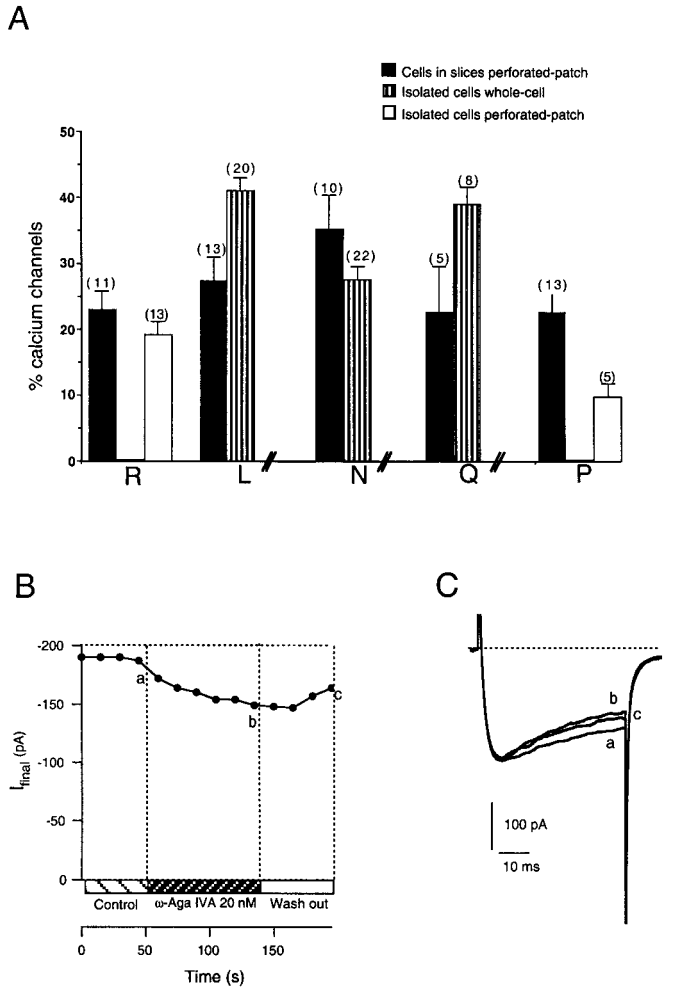

Figure 5. Relative contributions of Ca^{2+} channel subtypes to the whole-cell Ca^{2+} current. Data from recordings in the whole-cell configuration of the patch-clamp technique in isolated cultured mouse chromaffin cells are compared to those from recordings in the perforated-patch configuration in chromaffin cells of mouse adrenal slices or isolated in culture. *A*, *Black bars* represent the data obtained from cells of adrenal medullary slices in the perforated-patch configuration (this study); *bars* with *lines* are data from isolated cells kept in culture in the whole-cell configuration (Hernández-Guijo et al., 1998); *white bars* represent data of R- and P-type channels from isolated cells recorded in the perforated-patch configuration (this study). *B,* Time course of Ca^{2+} current blockade induced by 20 nM ω-Aga IVA, measured at the end of 50 msec depolarizing pulses to 0 mV, applied to a mouse chromaffin cell cultured for 2 d, under the perforated-patch configuration. The corresponding original traces for control conditions (*trace a*), in the presence of 20 nM ω-Aga IVA (*trace b*), or after wash out (*trace c*) are shown in *C*.

as a charge carrier and the perforated-patch technique were used, with values obtained in a previous study in mouse chromaffin cells maintained in culture, where 2 mM Ba^{2+} as a charge carrier and the whole-cell configuration were used (Hernández-Guijo et al., 1998). R-type channels are defined as the percentage of total Ca^{2+} channels remaining after the addition of the whole cocktail of blockers; P-type channels, Q-type channels, L-type channels, and N-type channels as the percentage of total Ca^{2+} channels blocked by 20 nM ω-Aga-IVA, 2 μM ω-Aga-IVA, 3 μM Nife, and 1 μM ω-CTx-GVIA, respectively, measured at the end of 50 msec depolarizing pulses. Note that with these definitions, the percent values do not add up to 100 because of small overlaps in the action of toxins.

Two types of channels present in adrenal slice cells recorded in the perforated-patch configuration were absent in cultured cells recorded in the whole-cell configuration: the R-type channel (22 ± 2.6%; $n = 11$ cells) and the P-type channel (22.4 ± 4%; $n = 13$ cells). Moreover, the proportion of L-type and "Q-like" Ca^{2+} channels was smaller in adrenal slice cells when compared to isolated cells: 27 ± 4% ($n = 13$ cells) and 22.6 ± 7% ($n = 6$ cells) for L- and "Q-like" channels in adrenal slice cells versus 41 ± 2% ($n = 40$ cells) and 39 ± 2.5% ($n = 35$ cells) in cultured cells. On the other hand, the proportion of N-type Ca^{2+} channels was similar: 35 ± 5% ($n = 12$ cells) in adrenal slices and 27.4 ± 2% ($n = 25$ cells) in cultured cells. The proportion of N-type Ca^{2+} channels in adrenal slice cells may be overestimated, because the effect of ω-CTx-GVIA in these cells was partially reversible. This might indicate that the toxin was blocking other Ca^{2+} channels, as described for other cell preparations (Kasai et al., 1987; Aosaki and Kasai, 1989).

We further investigated the presence of P- and R-type channels in isolated cells under the perforated-patch configuration. They could be recorded under this experimental condition, contrary to results obtained in previous studies in the whole-cell configuration. As the Figure 5*A* shows, P- and R-type channels accounted for 19.5 ± 2% ($n = 13$ cells) and 10 ± 3% ($n = 5$ cells) of the total current. These experiments are explained below.

P and resistant Ca^{2+} channels in mouse chromaffin cells maintained in culture

It was interesting to investigate if the lack of P- and R-type channels in mouse chromaffin cells maintained in culture as observed in previous studies could be caused by the whole-cell configuration used. We clarified this issue by performing new experiments in isolated mouse chromaffin cells in the perforated-patch configuration. ω-Aga-IVA (20 nM) blocked irreversibly 10 ± 3% of the control current at the end of the 50 msec depolarizing control pulse, but not the peak current (Fig. 5*B,C*) ($n = 5$ cells). In adrenal slice cells, however, the blockade by 20 nM ω-Aga-IVA was parallel to the control current, and reversible, indicating that culture conditions also affect the expression of Ca^{2+} channels.

We also investigated the existence of an R-type channel in mouse chromaffin cells maintained in culture under the same conditions as the ones used here for slice experiments. Figure 6*A* shows the time course of the current, elicited at the end of 50 msec depolarizing pulses, in a mouse chromaffin cell maintained for 1 d in culture, under the perforated-patch configuration. BBS-based solutions were used as external recording solution in this experiment. A cocktail of Ca^{2+} channel blockers composed of ω-CTX-GVIA (1 μM), ω-CTX-MVIIC (3 μM), Nife (3 μM), and ω-Aga-IVA (2 μM) blocked the control current within 15 sec, leaving a resistant component after 2 min of perfusion with the cocktail, which represents 19% of the total current. This resistant component was rapidly inhibited by $CdCl_2$ (200 μM). Original traces corresponding to control (*trace a*), cocktail (*trace b*), $CdCl_2$ (*trace c*), and wash out conditions (*trace d*) are shown in Figure 6*B*. In 13 cells tested, the resistant current amounted to 28.7 ± 2%, measured at the peak current and 19.5 ± 2%, measured at the end of the pulse.

Because previous studies that missed the resistant current used a HEPES-based solution to record Ca^{2+} currents, we investigated if the BBS-based solution might be the reason for the observation of a Ca^{2+} current resistant to blockade. Figure 6, *C* and *D,* shows that with HEPES-buffered solutions there was still a resistant current, which represented 22 ± 3%, measured at the peak current and 13.6 ± 3%, measured at the end of the pulse ($n = 10$ cells).

We also performed parallel experiments in the whole-cell configuration, superfusing cells with a HEPES-based solution, and found that the resistant current was slowly dialyzed, and almost disappeared after 2.5 min of the whole-cell recording (Fig. 6*E,F*) in four of five cells tested, with only 5% of resistant current remaining in those cells.

DISCUSSION

Similar to previous studies performed in cultured adrenal chromaffin cells of various species (for review, see García et al., 1997), we

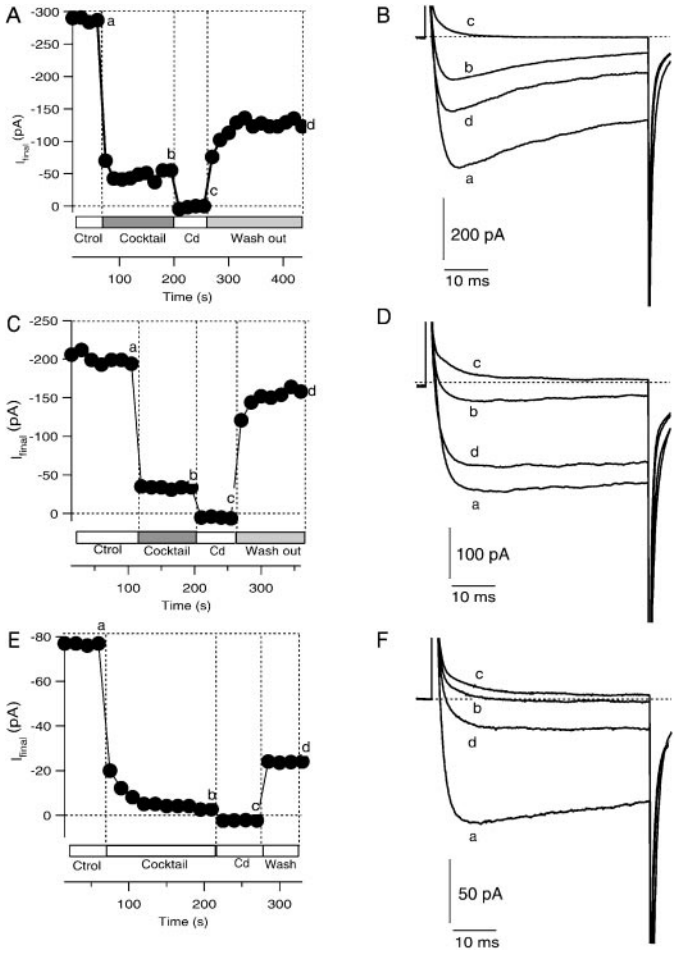

Figure 6. The resistant channel in isolated cultured mouse chromaffin cells. The time course of blockade for each experimental condition is shown in *A*, *C*, and *D*, and the corresponding original traces in the steady-state after superfusion of different solutions (*trace a* for the control condition, *trace b* for the cocktail, *trace c* for cadmium, and *trace d* for wash-out) are shown in *B*, *D*, and *F*. The same cocktail of blockers as in Figure 4*B–E* was used in these experiments. The perforated-patch configuration and BBS-based solutions were used in *A* and *B*. The perforated-patch configuration and HEPES-based solutions were used to record Ca^{2+} currents in *C* and *D*, and the whole-cell configuration and HEPES-based solutions were used in *E* and *F*. A residual current slowly disappeared in this cell, which was from the same culture as those cell of *C* and *D*.

have found here that mouse adrenal slice chromaffin cells express L-, N-, P-, and Q-subtypes of Ca^{2+} channels. However, contrary to all previous studies, we have found an R-type Ca^{2+} channel that accounts for a prominent component of I_{Ca} (~20%) and that is tightly coupled to the exocytotic release of catecholamines. This pronounced difference could be attributable to various factors: (1) the use of different extracellular solutions; (2) the use of adrenal slices; and (3) the use of the perforated-patch configuration.

Work aimed at characterizing ion currents in brain slices is usually done in BBS buffer equilibrated with carbogen (Wheeler et al., 1994; Wu et al., 1998). However, all previous studies in cultured chromaffin cells had been performed in HEPES-based solutions lacking bicarbonate and phosphate. Recently, the solution structure of ω-conotoxin MVIID, an analog of ω-CTx-MVIIC as far as blockade of N and P/Q channels is concerned, was determined (Civera et al., 1999). In this study it was found that positive and negative hydrophilic groups distribute in different areas of the molecule, so that ω-toxins behave as a dipole. This might profoundly influence the binding of toxins to their receptor in solutions of different ionic strength and composition. Thus, it might be that bicarbonate and phosphate anions could interfere with the binding of toxins as well. We re-evaluated that possibility by performing new experiments in the perforated-patch configuration using a HEPES-based solution as external solution. We ruled out that this is the cause for the R-type current discovered in this study, because in isolated cultured cells, the R component was present irrespective of the type of solution used (Fig. 6*A–D*).

Neither did the use of adrenal slices versus cultured cells seem to be the reason for the presence of R-type currents, because we found a clear R-type component in both adrenal slice and cultured cells when using the perforated-patch configuration (Figs. 4, 6*A–D*). Noteworthy, when the whole-cell configuration was used, the R-component was missed in all species studied so far (Fig. 6*E,F*) (Gandía et al., 1993, 1995, 1998; Albillos et al., 1994, 1996; Artalejo et al., 1994; Kitamura et al., 1997; Hernández-Guijo et al., 1998;). Only Hollins and Ikeda (1996), Currie and Fox (1996), and Prakriya and Lingle (1999) found a fraction of the total current that was resistant to blockade by DHP and ω-toxins in isolated chromaffin cells. However, 10 mM Ca^{2+} or 10 mM Ba^{2+} was used as a charge carrier in those studies, and it had previously been shown that the binding of toxins is extremely affected by the concentration of the charge carrier (Albillos et al., 1996; McDonough et al., 1996; Gandía et al., 1997). Thus, the recording configuration seemed to be critical for uncovering the R-type current. This means that some cytosolic factors are crucial for the activation of R-type channels in chromaffin cells. A different isoform of the channel might exist in neurons, because R-type channels had been recorded in the whole-cell configuration, using 2 mM Ca^{2+} as a charge carrier, in a rat central synapse (Wu et al., 1998).

Mouse chromaffin cells *in situ* exhibit a fast component of secretion that is hardly detectable in isolated cells. This fast secretory component originates from a small pool of vesicles situated in close proximity to Ca^{2+} channels. The secretory response to 50 msec depolarizations is composed mainly of the rapid component, which represents ~75% of the total response (Moser and Neher, 1997; Voets et al., 1999). Ca^{2+} entry through the resistant channel is responsible for half of the response evoked by 50 msec depolarizing pulses, thus suggesting a particularly tight coupling of this channel to the exocytotic machinery. Activation of R-type Ca^{2+} channels evokes neurotransmitter release in the mammalian CNS (Wu et al., 1998; Wang et al., 1999). However, Ca^{2+} influx via R-type Ca^{2+} channels triggers secretory responses less effectively than that via N- and P/Q-type Ca^{2+} channels. This might be attributable to the fact that in neurons a substantial fraction of R-type Ca^{2+} channels is localized at some distance from release sites, as demonstrated by immunocytochemical staining experiments performed in presynaptic terminals of a calyx-type synapse (Wu et al., 1999). Recent data have also demonstrated that R-type Ca^{2+} channels preferentially regulate oxytocin release from neurohypophysial terminals (Wang et al., 1999).

Concerning the other Ca^{2+} channel subtypes, we also found interesting differences between adrenal slices and cultured cells. For instance, the P-type Ca^{2+} channel was absent in isolated mouse chromaffin cells kept in culture (Hernández-Guijo et al., 1998). The present results indicate that 20 nM ω-agatoxin IVA blocked 22% of the total current in adrenal slice cells. Higher concentrations of the toxin (2 μM) caused a further blockade of 22% of Ca^{2+} current. This value is substantially smaller than the 39% found for the Q-type channel in isolated cells, using the whole-cell configuration of the patch-clamp technique (Hernández-Guijo et al., 1998). No comparison can be performed regarding inactivation kinetics because Ba^{2+} was the charge carrier ion in this latter study. Similar to the neuronal P channel (Usowicz et al., 1992; Randall and Tsien, 1995), P-type channels described here did not inactivate. Q channels are prominently inactivating in neurons (Mintz et al., 1992a; Randall and Tsien, 1995) or in currents supported by α_{1A} subunits expressed in *Xenopus* oocytes (Sather et al., 1993). However, the Ca^{2+} current sensitive to high concentrations of ω-agatoxin IVA in adrenal slice chromaffin cells did not display any inactivation.

P-type Ca^{2+} channels were also investigated in the present study

under the perforated-patch configuration to analyze if, similarly to R-type Ca^{2+} channels, their presence in isolated mouse chromaffin cells was missed because of the patch-clamp configuration used. ω-Aga-IVA (20 nM) blocked almost irreversibly the control current by 10%, sharply increasing the inactivation of the current, at variance with the blockade observed in mouse chromaffin cells *in situ*, where the toxin blockade was reversible and did not uncover inactivation. This indicates that culture conditions might also affect the expression and kinetic properties of channels, as previously observed when comparing adult Purkinje cells maintained in culture with Purkinje cells in brain slices (Bossu et al., 1989; Usowicz et al., 1992). Thus, our present data suggest that the recording configuration as well as culture conditions are of critical relevance for the properties of Ca^{2+} currents and secretion control.

The amount of I_{Ca} blockade exerted by ω-conotoxin GVIA in our study in slices was similar to that found in studies on isolated cells. A major difference was the partial reversibility of the blockade by the toxin in cells of adrenal slices, which amounted to half the blockade. This reversibility has been observed before in cultured cat chromaffin cells (Albillos et al., 1994) and in neurons (Kasai et al., 1987; Aosaki and Kasai, 1989), and could reflect the binding of the toxin to some other Ca^{2+} channels, as described for other cell preparations (Kasai et al., 1987; Aosaki and Kasai, 1989), or to different isoforms of N-type Ca^{2+} channels. In fact, molecular biology techniques revealed the expression in bovine chromaffin cells of different isoforms of N-type Ca^{2+} channels (Cahill et al., 2000).

The contribution of L-type Ca^{2+} channels to the total current was also quite different between cells in adrenal slices and cells maintained in culture, accounting, in this case, for 27 and 41%, respectively. The resolution of our recordings did not allow to measure the relative contribution of the different non R-type Ca^{2+} channels to the fast secretory component.

In conclusion, we provide the first demonstration for the presence, in mouse adrenal slice chromaffin cells, of R-type Ca^{2+} channels, that are tightly coupled to the control of their rapid secretory response. In addition, we found pronounced differences between the relative proportions of L-, N-, P-, and Q-type Ca^{2+} channels expressed by chromaffin cells in the intact tissue, and in cultured cells.

REFERENCES

Albillos A, García A, Gandía L (1993) ω-Agatoxin-IVA-sensitive calcium channels in bovine chromaffin cells. FEBS Lett 336:259–262.

Albillos A, Artalejo AR, López MG, Gandía L, García AG, Carbone E (1994) Ca^{2+} channel subtypes in cat chromaffin cells. J Physiol (Lond) 477:197–213.

Albillos A, García AG, Olivera B, Gandía L (1996) Re-evaluation of the P/Q Ca^{2+} channel components of Ba^{2+} currents in bovine chromaffin cells superfused with solutions containing low and high Ba^{2+} concentrations. Pflügers Arch 432:1030–1038.

Aosaki T, Kasai H (1989) Characterization of two kinds of high-voltage-activated Ca-channel currents in chick sensory neurons. Differential sensitivity to dihydropyridines and ω-conotoxin GVIA. Pflügers Arch 414:150–156.

Artalejo CR, Perlman RL, Fox AP (1992) ω-Conotoxin GVIA blocks a Ca^{2+} current in chromaffin cells that is not of the "classic" N Type. Neuron 8:85–95.

Artalejo CR, Adams ME, Fox AP (1994) Three types of Ca^{2+} channels trigger secretion with different efficacies in chromaffin cells. Nature 367:72–76.

Bossu JL, Dupont JL, Feltz A (1989) Calcium currents in rat cerebellar Purkinje cells maintained in culture. Neuroscience 30:605–617.

Bossu JL, De Waard M, Feltz A (1991a) Inactivation characteristics reveal two calcium currents in adult bovine chromaffin cells. J Physiol (Lond) 437:603–620.

Bossu JL, De Waard M, Feltz A (1991b) Two types of calcium channels are expressed in adult bovine chromaffin cells. J Physiol (Lond) 437:621–634.

Cahill AL, Hurley JH, Fox AP (2000) Coexpression of cloned α_{1B}, β_{2a}, and α_2/δ subunits produces non-inactivating calcium currents similar to those found in bovine chromaffin cells. J Neurosci 20:1685–1693.

Carbone E, Lux HD (1987) Kinetics and selectivity of a low-voltage-activated calcium current in chick and rat sensory neurones. J Physiol (Lond) 386:547–570.

Civera C, Vázquez A, Sevilla JM, Bruix M, Gago F, García AG, Sevilla P (1999) Solution structure determination by two-dimensional ^{1}H-NMR of ω-conotoxin MVIID, a calcium channel blocker peptide. Biochem Biophys Res Commun 254:32–35.

Currie KPM, Fox AP (1996) ATP serves as a negative feedback inhibitor of voltage-gated Ca channel currents in cultured bovine adrenal chromaffin cells. Neuron 16:1027–1036.

Gandía L, Albillos A, García AG (1993) Bovine chromaffin cells possess FTX-sensitive calcium channels. Biochem Biophys Res Commun 194:671–676.

Gandía L, Borges R, Albillos A, García AG (1995) Multiple types of calcium channels are present in rat chromaffin cells. Pflügers Arch 430:55–63.

Gandía L, Lara B, Imperial JS, Villarroya M, Albillos A, Maroto R, García AG, Olivera B (1997) Analogies and differences between ω-conotoxins MVIIC and MVIID: binding sites and functions in bovine chromaffin cells. Pflügers Arch 435:55–64.

Gandía L, Mayorgas I, Michelena P, Cuchillo I, de Pascual R, Abad F, Novalbos JM, Larrañaga E, García AG (1998) Human adrenal chromaffin cell calcium channels: drastic current facilitation in cell clusters, but not in isolated cells. Pflügers Arch 436:696–704.

García AG, Albillos A, Gandía L, López MG, Michelena P, Montiel C (1997) Calcium channels and toxins. In: Cellular and molecular mechanisms of toxin action, Ed 2 (Lazarovici B, Gutman Y, eds), pp 155–209. Switzerland: Academic.

Gillis KD (1995) Techniques for membrane capacitance measurements. In: Single-channel recording, Ed 2 (Sackmann B, Neher E, eds), pp 155–198. New York: Plenum.

Grantham CJ, Bowman D, Bath CP, Bell DC, Bleakman D (1994) ω-Conotoxin MVIIC reversibly inhibits a human N-type calcium channel and calcium influx into chick synaptosomes. Neuropharmacology 33:255–258.

Hans M, Illes P, Takeda K (1990) The blocking effects of ω-conotoxin on Ca^{2+} current in bovine chromaffin cells. Neurosci Lett 114:63–38.

Hernández-Guijo JM, de Pascual R, García AG, Gandía L (1998) Separation of calcium channel current components in mouse chromaffin cells superfused with low- and high-barium solutions. Pflügers Arch 436:75–82.

Hillyard DR, Monje VD, Mintz MI, Bean BP, Nadasdi L, Ramachandran J, Miljanich G, Azimi-Zoonooz A, McIntosh JM, Cruz LJ, Imperial JS, Olivera BM (1992) A new conus peptide ligand for mammalian presynaptic Ca^{2+} channels. Neuron 9:69–77.

Hollins B, Ikeda S (1996) Inward currents underlying action potentials in rat adrenal chromaffin cells. J Neurophysiol 76:1195–1211.

Horrigan FT, Bookman RJ (1994) Releasable pools and the kinetics of exocytosis in adrenal chromaffin cells. Neuron 13:1119–1129.

Hoshi T, Smith SJ (1987) Large depolarization induces long openings of voltage-dependent calcium channels in adrenal chromaffin cells. J Neurosci 7:571–580.

Kasai H, Aosaki T, Fukuda J (1987) Presynaptic Ca-antagonist ω-conotoxin irreversibly blocks N-type Ca channels in chick sensory neurons. Neurosci Res 4:228–235.

Kitamura N, Ohta T, Ito S, Nakazato Y (1997) Calcium channels subtypes in porcine adrenal chromaffin cells. Pflügers Arch 434:179–187.

López MG, Villarroya M, Lara B, Martínez-Sierra R, Albillos A, García AG, Gandía L (1994) Q- and L-type Ca^{2+} channels dominate the control of secretion in bovine chromaffin cells. FEBS Lett 349:331–337.

Magnelli V, Baldelli P, Carbone E (1998) Antagonists-resistant calcium currents in rat embryo motoneurons. Eur J Neurosci 10:1810–1825.

McDonough SI, Swartz KJ, Mintz IM, Boland LM, Bean BP (1996) Inhibition of calcium channels in rat central and peripheral neurons by omega-conotoxin MVIIC. J Neurosci 16:2612–2623.

Mintz IM, Adams ME, Bean BP (1992a) P-type calcium channels in rat central and peripheral neurons. Neuron 9:85–95.

Mintz IM, Venema VJ, Swiderek K, Lee T, Bean BP, Adams ME (1992b) P-type calcium channels blocked by the spider toxin ω-Aga-IVA. Nature 355:827–829.

Moser T (1998) Low conductance intercellular coupling between mouse chromaffin cells in situ. J Physiol (Lond) 506:195–205.

Moser T, Neher E (1997) Rapid exocytosis in single chromaffin cells recorded from mouse adrenal slices. J Neurosci 17:2314–2323.

Park YB (1994) Ion selectivity and gating of small conductance Ca^{2+}-activated K^+ channels in cultured rat adrenal chromaffin cells. J Physiol (Lond) 481:555–570.

Prakriya M, Lingle CJ (1999) BK channel activation by brief depolarizations requires Ca influx through L- and Q-type Ca channels in rat chromaffin cells. Am Physiol Soc 81:2267–2278.

Randall A, Tsien RW (1995) Pharmacological dissection of multiple types of Ca^{2+} channel currents in rat cerebellar neurons. J Neurosci 15:2995–3012.

Sather WA, Tanabe T, Zhang J-F, Mori Y, Adams ME, Tsien RW (1993) Distinctive biophysical and pharmacological properties of class A (BI) calcium channel α_1 subunits. Neuron 11:291–303.

Swartz KJ (1993) Modulation of Ca^{2+} channels by protein kinase C in rat central and peripheral neurons: disruption of G-protein-mediated inhibition. Neuron 11:305–320.

Tottene A, Moretti A, Pietrobon D (1996) Funtional diversity of P-type and R-type calcium channels in rat cerebellar neurons. J Neurosci 16:6353–6363.

Usowicz MM, Sugimori M, Cherksey B, Llinás R (1992) P-type calcium channels in the somata and dendrites of adult cerebellar Purkinje cells. Neuron 9:1185–1199.

Voets T, Neher E, Moser T (1999) Mechanisms underlying phasic and sustained secretion in chromaffin cells from mouse adrenal slices. Neuron 23:607–615.

Wang G, Dayanithi G, Newcomb R, Lemos JR (1999) An R-type Ca^{2+} current in neurohypophysial terminals preferentially regulates oxytocin secretion. J Neurosci 19:9235–9241.

Wheeler DB, Randall A, Tsien RW (1994) Roles of N-type and Q-type Ca^{2+} channels in supporting hippocampal synaptic transmission. Science 264:107–111.

Wu LG, Borst G, Sakmann B (1998) R-type Ca^{2+} currents evoke transmitter release at a rat central synapse. Proc Natl Acad Sci USA 95:4720–4725.

Wu LG, Westenbroek RE, Borst JGG, Catterall WA, Sakmann B (1999) Calcium channel types with distinct presynaptic localization couple differentially to transmitter release in single calyx-type synapses. J Neurosci 19:726–736.

Zhang J-F, Randall AD, Ellinor PT, Horne WA, Sather WA, Tanabe T, Schwarz TL, Tsien RW (1993) Distinctive pharmacology and kinetics of cloned neuronal Ca^{2+} channels and their possible counterparts in mammalian CNS neurons. Neuropharmacology 32:1075–1088.